Response of snow cover and runoff to climate change in high Alpine catchments of Eastern Switzerland

M. Bavay[a,*], T. Grünewald[a,b], M. Lehning[a,b]

[a] *WSL Institute for Snow and Avalanche Research SLF, Flüelastrasse 11, CH-7260 Davos Dorf, Switzerland*
[b] *CRYOS School of Architecture, Civil and Environmental Engineering, École Polytechnique Fédérale de Lausanne, Lausanne, Switzerland*

Abstract

A model study on the impact of climate change on snow cover and runoff has been conducted for the Swiss Canton of Graubünden. The model Alpine3D has been forced with the data from 35 Automatic Weather Stations in order to investigate snow and runoff dynamics for the current climate. The data set has then been modified to reflect climate change as predicted for the 2021-2050 and 2070-2095 periods.

The predicted changes in snow cover will be moderate for 2021-2050 and become drastic in the second half of the century. Towards the end of the century the snow cover changes will roughly be equivalent to an elevation shift of 800 m. Seasonal snow water equivalents will decrease by one to two thirds and snow seasons will be shortened by five to nine weeks in 2095.

Small, higher elevation catchments will show more winter runoff, earlier spring melt peaks and reduced summer runoff. Where glacierized areas exist, the transitional increase in glacier melt will initially offset losses from snow melt. Larger catchments, which reach lower elevations will show much smaller changes since they are already dominated by summer precipitation.

Keywords: Climate Change, Snow Cover, Modeling Future Runoff, Water Resources, Snow Melt, Catchment Hydrology

*Phone: +41 81 4170 265
Email address: bavay@slf.ch (M. Bavay)

1. Introduction

The adaption to global climate change often requires very local action and thus local information on future changes, which is often not available. One example is the increased demand for irrigation water in a warmer and potentially dryer future climate [1], which may generate conflicts of interest with other water uses such as electricity production or may cause severe ecological consequences [2]. In particular areas in southern Europe and central Asia may be heavily affected but even traditionally water rich areas in the North start to become concerned about future water use.

We investigate the local response of the high alpine catchments in the canton of Graubünden in Eastern Switzerland to predicted climate change. The runoff dynamics in most of these catchments are dominated by snow storage and comparable to other snow dominated catchments e.g. in the Sierra Nevada of California [3]. While it has been recognized quite early that the snow cover may be particularly vulnerable to climate change [4, 5, 6, 7] and that the snow cover dynamics heavily influence runoff dynamics [8, 9] most studies concentrate on glacier dynamics and their hydrological consequences [10, 11, 12, 13]. The current study focuses on the snow cover dynamics in a high alpine area in central Europe.

The novelty of our study lies in the fact that with the same physically based model approach of Alpine3D [14] predictions are made for 48 catchments in Graubünden, which include small high altitude headwater catchments and the larger main catchments of Inn and Rhine, the latter extending to much lower altitudes. This allows to assess the change over a variety of catchments with different characteristics. The physically based approach should have advantages in simulating heavily changed snow dynamics in the future including changes in evaporation [15]. It is generally agreed that heavily parameterized models are less reliable if used for extrapolation to different climatic conditions then models that are physics based.

This paper first introduces the methods in Section 2 with an overview of the study domain, the climate change scenarios used and the modeling approach. In Section 3, the results are presented with respect to Snow Water Equivalent (SWE) changes, snow season changes and runoff generation changes. A particular focus is the change in contribution from rain, snow melt and ice melt. Finally, in Section 4, the results are further interpreted and discussed in light of uncertainties inherent of model studies of this kind.

2. Methods

In this section, we will describe the domain that has been chosen as well as the selection and preparation of the input data and the detailed setup of the model.

2.1. Domain

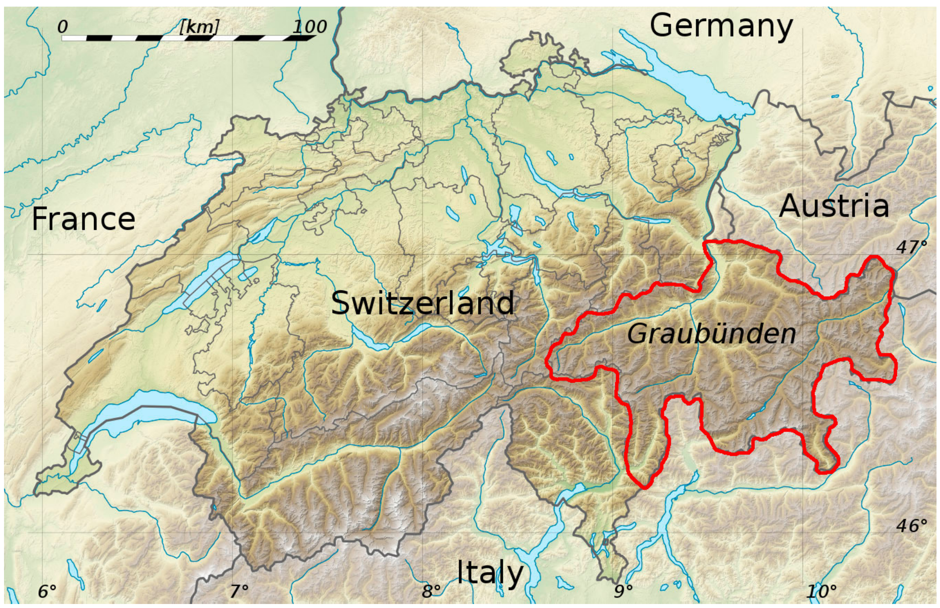

Figure 1: Geographical situation of the domain of interest. Base map ©2004 SwissTopo.

This study investigates the canton Graubünden, in Eastern Switzerland (see Figure 1). It covers 7214 km^2 with elevations ranging from 250 m a.s.l to 4049 m a.s.l with a mean elevation of 1853 m a.s.l as shown in Figure 2. This domain is dominated by mountains and contains the catchments of the Upper Rhine and the Inn. Glaciers cover 2.4 % of the total area. Some high elevation catchments have up to 20 % of their total surface covered by glaciers (catchments 5, 42, 21 – see individual catchments in Figure 5) while the average elevation of glaciers in the whole domain is 2900 m a.s.l (see Figure 4).

The average temperature and weekly precipitation at two Automatic Weather Stations (AWS) located in the Upper Rhine catchment (Chur station) and in the Inn catchment (Samedan station) are shown in Figure 3.

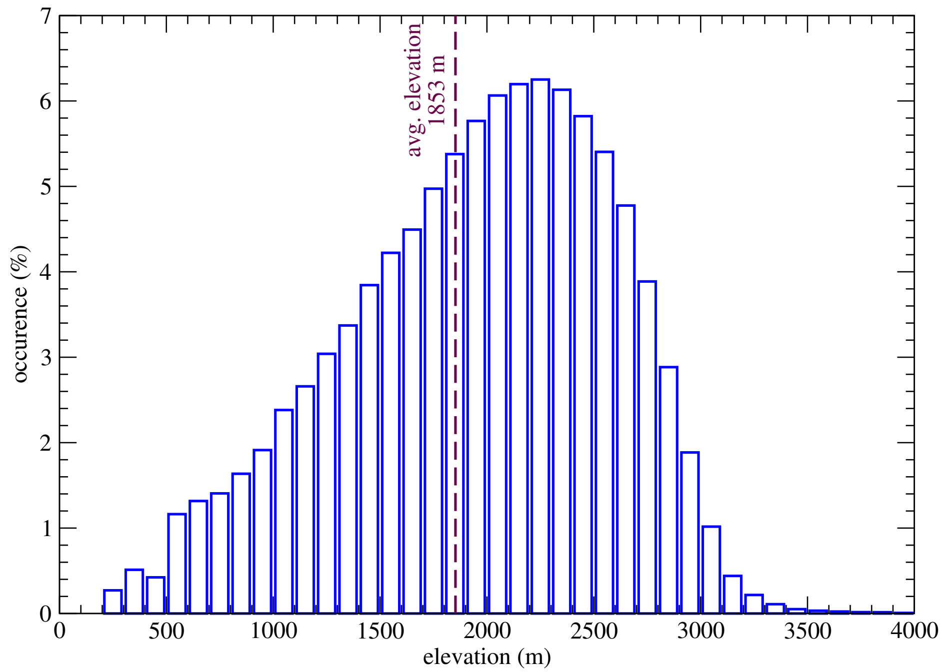

Figure 2: Distribution of the elevations in the modeled domain, by classes of 100 m

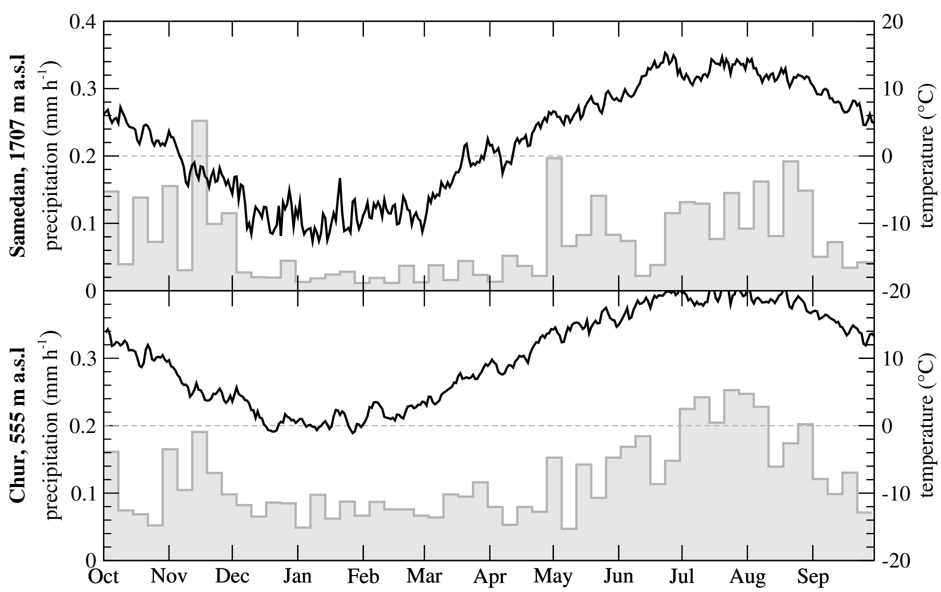

Figure 3: Average weekly precipitation and daily temperature in southern Graubünden (Samedan, 1707 m a.s.l) and northern Graubünden (Chur station, 555 m a.s.l) for 2001 to 2010.

Both stations are on valley floors but the two catchments cover different elevation ranges: the Upper Rhine is a low elevation valley (from 250 m a.s.l. to 3614 m a.s.l., valley floor at around 700 m a.s.l.) that drains most of the northern part of the modeled domain while the Inn is a relatively high elevation valley (from 1035 to 4049 m a.s.l, valley floor at around 1600 m a.s.l.) that drains the southern and smaller part of the domain. As it can be seen from the climatology, the Inn catchment is dryer than the Rhine, especially in spring and summer.

2.2. Input Data

The domain has been simulated with a standard 200 m horizontal resolution Digital Elevation Model (DEM). This defines the simulation grid that has to be filled with land cover data and downscaled meteorological input data for each cell for the time period of interest at an hourly resolution.

2.2.1. Meteorological Data

The reference data set consists of AWS data from the IMIS and ANETZ monitoring networks jointly operated by the Swiss office for meteorology (MeteoSwiss) and the WSL Institute for Snow and Avalanche Research [16]. Stations were selected based on the requirement that they provide hourly meteorological data and are located in or close to the simulation domain. The following meteorological variables are necessary for the model:

- air temperature
- relative humidity
- wind velocity
- precipitation
- incoming longwave radiation
- incoming shortwave radiation

In fact, in its current form, the model only uses one incoming shortwave radiation measurement per time step for the whole domain with air temperature and relative humidity measured at the same point, in order to compute the effects of the atmosphere on radiation (such as attenuation and diffusion but excluding the terrain effects that are computed separately, see Section

2.3.1). For the non radiation parameters, we have a set of 35 AWS that provide hourly data, including 12 stations equipped with rain gauges. In order to keep the computational time manageable and data availability optimal, simulations have only been made for ten years. The incoming longwave radiation was only available from one station of the World Radiation Center (WRC) in Davos and was therefore assumed to only depend on elevation.

All parameters have then been spatially interpolated to fill the simulation grid as defined by the DEM using the data access and pre-processing library MeteoIO [17]. The interpolations were computed using an Inverse Distance Weighting (IDW) with elevation lapse rate for air temperature, IDW for precipitation, IDW with elevation lapse rate for wind velocity and an elevation corrected value for incoming longwave radiation. All lapse rates, except for incoming longwave radiation, were recomputed on the fly for each time step by a robust linear regression on the data. This consisted in excluding the data points degrading the linear regression the most, one by one, if the correlation coefficient would drop below 0.7, until either the correlation coefficient would be greater than 0.6 or 15 % of the initial data set would have been excluded. The incoming longwave radiation was computed with a fixed elevation lapse rate of -0.03125 $W/m^2/m$ that represents a yearly average in this area for this parameter [18]. The relative humidity was computed by converting it to a dew point temperature, then interpolating it with IDW with an elevation lapse rate and recomputing the local relative humidity, as also suggested by Liston and Elder [19].

2.2.2. Climate Scenarios and Downscaling

The climate scenarios have been taken from the Swiss Climate Change Scenarios CH2011 [20] based on the IPCC A1B emission scenario [21]. This data set contains daily averages of deltas (i.e. the average daily difference between the reference period and a given scenario for the air temperature and as a scaling factor for the precipitation) suitable for use in a simplified delta change method (Graham et al. [22], Bosshard et al. [23]) from ten different Regional Climate Models (RCM). The values are available for all stations of the Swiss monitoring networks and are nominally valid for average years of the periods 2021-2050 and 2070-2095. These deltas consist of a temperature offset ΔT and a precipitation scaling factor k_P as shown in Figure 4.

These spatially distributed deltas have been investigated and no elevation dependency was found between the deltas for the selected stations. This means that the resolution of the RCM was not high enough to properly simulate the mountains of the domain, and accordingly their impact on spatial distribution. Therefore, the spatial average of the deltas for all the selected stations has been computed, one for each scenario and each period. This defines the climate change signal.

In order to present a range of possible scenarios within the general IPCC A1B emissions scenario, out of ten RCMs, three have been chosen for a low (BCM), medium (ARPEGE) and high (ETH) temperature change (see Table 1). These have been selected for the magnitude of changes they project as well as for their usage in partner studies (e.g. CCHydro, Swiss Federal Office for Environment; Climate Change and Hydropower Generation, Kobierska et al. [24]; Interreg CLISP (http://www.clisp.eu)). The annual mean changes are shown in Table 2 while the daily variations are shown in Figure 4.

Scenario	**GCM**	**RCM**	**Institution**
BCM	BCM	RCA	Swedish Meteorological and Hydrological Institute
ARPEGE	ARPEGE	ALADIN	Centre National de Recherches Météorologiques
ETH	HadCM3Q0	CCLM	Eidgenössische Technische Hochschule Zürich

Table 1: Abbreviations, Global Climate Models (GCM) and Regional Climate Models (RCM) used for the future meteorological scenarios.

Year	**Scenario**	**ΔT [°C]**	**precipitation factor k_P**
2050	BCM	0.58	1.005
	ARPEGE	1.21	0.998
	ETH	1.9	0.971
2095	BCM	2.24	0.966
	ARPEGE	3.08	0.912
	ETH	3.9	0.951

Table 2: Average change for the selected scenarios for the 2021-2050 and 2070-2095 periods.

The reference simulation covers the time period 2000-10-01 to 2010-07-21 with the measured meteorological data of 35 stations. The scenarios for the period 2021-2050 and 2070-2095, respectively, run on the same data set where the delta change signals were applied to the air temperatures and the precipitation. This is a very close to the approach of Bavay et al. [8], except that the deltas have been directly applied to the hourly values instead of working by deciles over a given period of integration.

2.2.3. Glaciers and Land Cover

The glacier changes for these future climate scenarios have been incorporated on the basis of the glacier modeling by Paul et al. [25]. Departing from an assessment of glacier extent for the current climate, for both periods (2021-2050 and 2070-2095) a low, moderate and high temperature increase scenario were used to generate three glaciers maps. The glaciated surfaces for the simulated domain in these scenarios are summarized in Table 3. The ice thickness for each glacier pixel should have been given by estimating the glacier volume [11]. This was impractical on such a large scale, so a fixed thickness has been attributed to each glacier pixel. Moreover, in order to compute a snapshot for each climate scenario as an average over 10 years, the glacier extent has to remain approximately constant over the simulation period. This has been achieved by providing each pixel with 80 m of ice in its initial state so that some ice would remain at the end of the period even for the pixels experiencing the most glacier melt.

Year	**Scenario**	**Glaciated Surface [km^2]**
2010	reference	172
2050	s2, low	99
	s3, moderate	92
	s4, high	87
2095	s2, low	56
	s3, moderate	31
	s4, high	20

Table 3: Glaciated surfaces for the reference, 2021-2050 scenarios and 2070-2095 scenarios

Digital land cover maps from the Swiss Federal Statistical Office [26] have been used which have been aggregated and converted from their original NOAS92_74 classification into Prevah land use codes [27], as necessary for the model. The loss of detail introduced by the conversion to a different classification system has a negligible impact on the simulation itself since the detailed tree or plant species information is not used by Alpine3D.

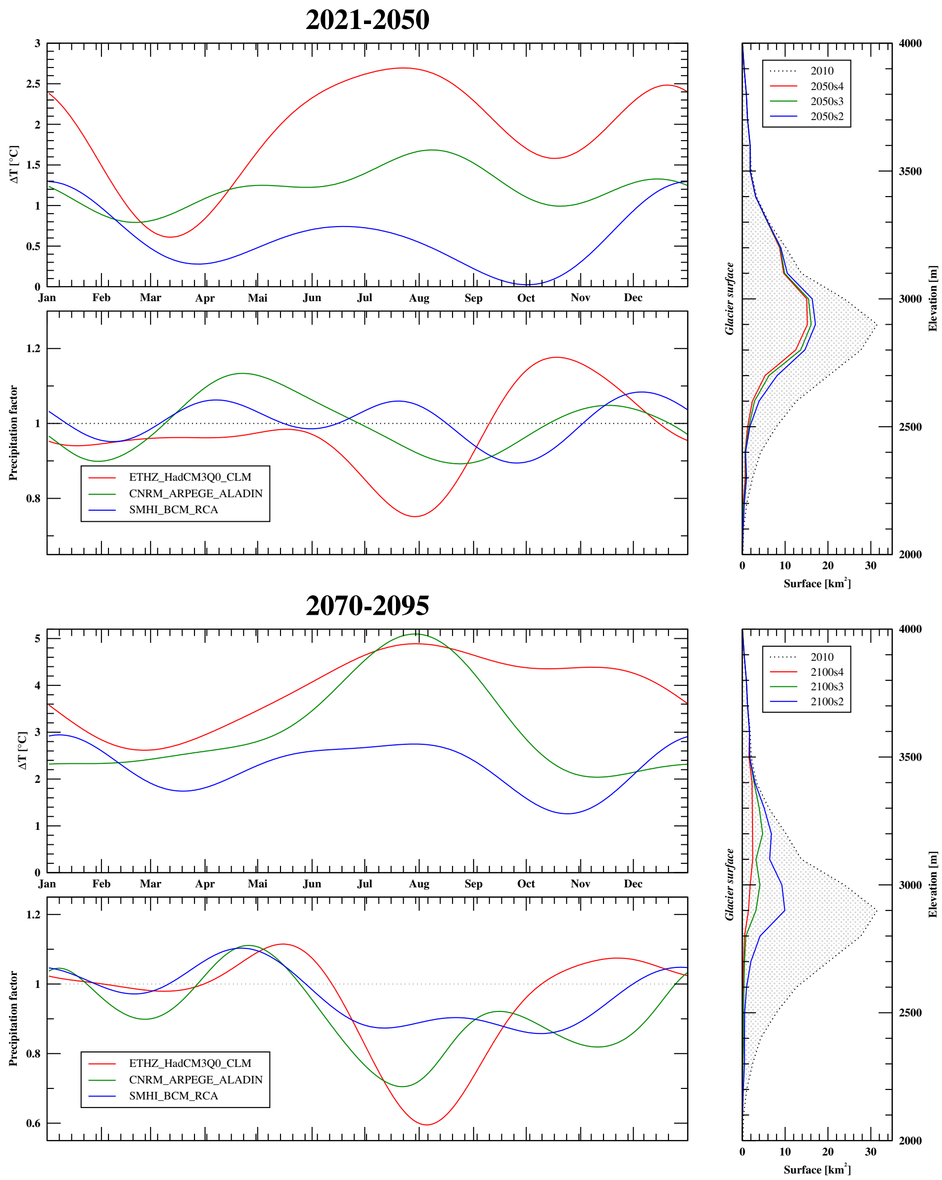

Figure 4: Climate and glacier extents scenarios for the 2021-2050 and 2070-2095 periods

2.3. Modeling setup

The modeling has been performed with the alpine surface processes model Alpine3D [14]. This model has been successfully used in the past for studies about climate change [8, 11], snow transport [28, 29], snow spatial distribution [30, 31], radiation balance [32], permafrost [33, 34] and glacier mass balance [35]. The model has been validated for simulating the reference period on a smaller area that is part of the current domain in a previous work [8] by looking at snow heights at various locations and catchment discharge.

The input data pre-processing has been delegated to the MeteoIO library [17], while Alpine3D computed the spatial distribution of shortwave radiation and simulated the snow cover distribution using the Snowpack model [36] by providing it with the local climatologic forcing (a detailed description of each step involved is given below).

2.3.1. Radiation modeling

The shortwave radiation fields have been computed by establishing a coefficient of attenuation in the atmosphere (compared to a clear sky atmosphere) from a point measurement at ground level and assuming that this coefficient is constant over the whole domain. The splitting coefficient between diffuse and direct radiation has also been computed at ground level, based on the point measurement. Then, each cell of the domain received the direct shortwave contribution with the elevation dependency of a standard atmosphere, corrected by the atmospheric attenuation coefficient, if the said pixel was not shaded by other pixels of the terrain. The diffuse component was assumed to be spatially constant.

2.3.2. Snow cover model

At each pixel of the modeled domain, a set of meteorological parameters is then available to perform a 1D simulation of the vegetation, snow, ice, soil column using the Snowpack model. This assumes that no lateral transport occurs in the soil/snow/canopy column and that all lateral flow occurs through the atmosphere or through water flow below the soil. Snowpack then performes a detailed energy and mass tranport simulation in the column using an arbitrary number of layers and various models for the canopy, snow, ice and soil compartments. It also simulates the melting of the snow cover and generates runoff in the snow, which is passed to lower snow or soil layers using a simple bucket model.

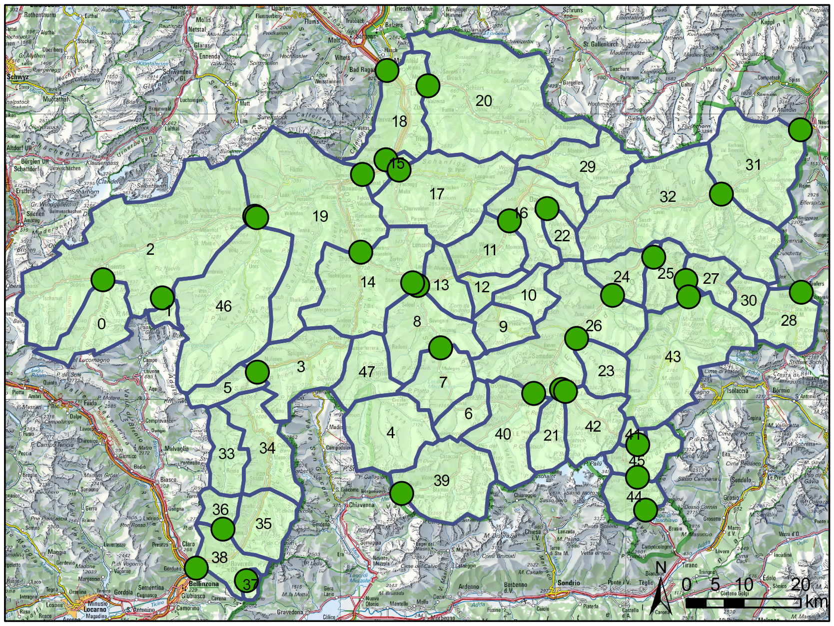

Figure 5: Division of the whole domain into 48 individual catchments, green dots representing existing gauging stations. Base map ©2009 SwissTopo.

At glaciated pixels, in the absence of snow on the glacier ice, the atmospheric stability was set to stable for air temperature above 5° Celsius [11]. The albedo of ice was also forced to a fixed value of 0.3, in order to prevent the albedo model for snow [37] from computing values inconsistent with known values for glacier ice albedo [38]. When the pixel was covered with snow on top of the glacier ice, none of the above settings was applied. This is consistent with what had been developed for a previous study by Kobierska et al. [24] which focuses on the hydrological aspect.

2.3.3. Runoff modeling

Since there is no detailed subsurface information for such a large area, the soil has been modeled for each pixel according to its land cover classification. It has been modeled with 19 layers over a depth of 25 m, with a finer layering close to the surface. This allowed to store runoff water in the soil as well as a proper simulation of permafrost effects (ice lenses, frozen soil). During snow melt season, the snow model calculated the melting of the snow pack and delivered melt water to the soil below. Any excess water that could not be stored in the soil for a given pixel was added to the runoff.

The domain has been divided in 48 individual catchments, providing 48 individual spatial runoff sums (see Figure 5). This division has been done according to topography and existing gauging stations, leading to some of these catchments being headwater catchments while some others only match a given section of a larger river. Moreover, the runoff was categorized per grid cell according to its origin:

- if the local air temperature was greater than a snow/rain threshold of 1.2° Celsius (standard value in Snowpack);
  - if the local precipitation was greater than the runoff, then the entire runoff was defined to originate from precipitation;
  - if the local precipitation was less than the runoff, then an amount equal to the precipitation was assumed to come from the precipitation with the remaining coming from melt
- if the local air temperature was below the snow/rain threshold, all local precipitation was assumed to be snow and any continuing runoff was categorized as melt

Glacier pixels provided glacier melt, even if only the seasonal snow was actually melting on the glacier. This definition has been chosen in order to be consistent with common practice in glacier hydrology. While this classification scheme is imperfect it seemed to be the best way to generate a spatio-temporally resolved classification of runoff origin.

2.3.4. Model parallelization

In order to keep the computation time manageable, the model has been parallelized [39]. Alpine3D splits the domain into bands of pixels that are given to Snowpack for computing the snow cover evolution for a given time step, then re-assembles them into full domain grids. Simulating almost ten years over the whole domain using 72 computing cores required 2-3 weeks. After parallelizing the radiation computation along the same lines, the same simulation only required approximately three days of computation.

3. Results and discussion

The results from the ten simulated years for the reference and for all scenarios have been averaged to build an approximate climatological year for a given scenario and time period. This lead to an intended smoothing of individual weather events, which are still present in the station data.

3.1. Snow Water Equivalent

Year	Scenario	Mean SWE [mm]	Absolute volumes [km^3]	Relative change [%] Vol.
2010	Reference	257	1.8	100
2050	BCM	235	1.6	89
	ARPEGE	204	1.4	78
	ETH	183	1.3	72
2095	BCM	167	1.2	67
	ARPEGE	130	0.9	50
	ETH	93	0.6	33

Table 4: Mean Snow Water Equivalent and absolute SWE volumes over the whole domain per scenario and per period compared to the current climate.

Figure 6 shows the average snow cover on April 15th (which is approximately the date of maximal snow water equivalent for the domain under the current climate) for each scenario and period. Dramatic changes are visible. The mean SWE as well as the total volume of water output (runoff) computed over the whole domain is shown in Table 4. Note that SWE is not accounted for at glaciated pixels because of the arbitrary ice thickness initialization as discussed in Section 2.2.3.

The SWE sums over the whole domain excluding the seasonal snow cover on the glaciers are shown in Figure 7 for each scenario and period.

For many alpine catchments, water stored in the snow pack represents a significant fraction of the overall yearly water output. Table 4 shows that even for the 2021-2050 period, a clear reduction of the total volume of SWE is visible, which ranges from 11 to 28 % for the various scenarios. For the 2070-2095 period, the effect becomes dramatic, with a reduction of up to 67 %. Figures 6 and 8 indicate that the storage of water in snow will particularly be reduced in the lower elevations. This is on the one hand due to an upward shift of the snow line and on the other hand due to an earlier and faster meltout of the snow cover. The general reduction of SWE in the accumulation season will lead to a reduction of the water available for runoff in spring and summer.

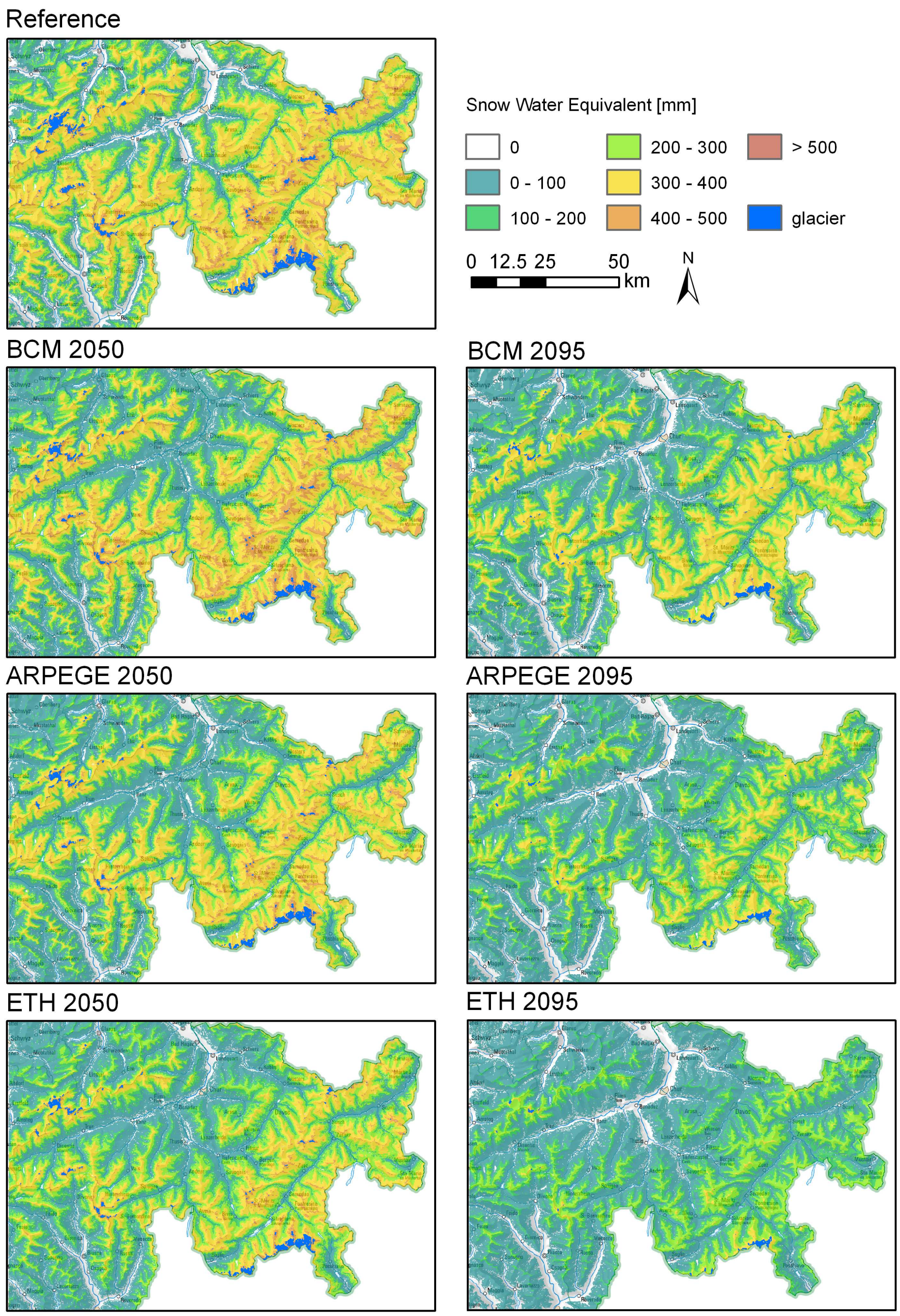

Figure 6: Mean Snow Water Equivalent for April 15th of an average year for the reference period as well as 2021-2050 and 2070-2095 scenarios. Glaciers (blue areas) were excluded from statistics as shown in Table 4.

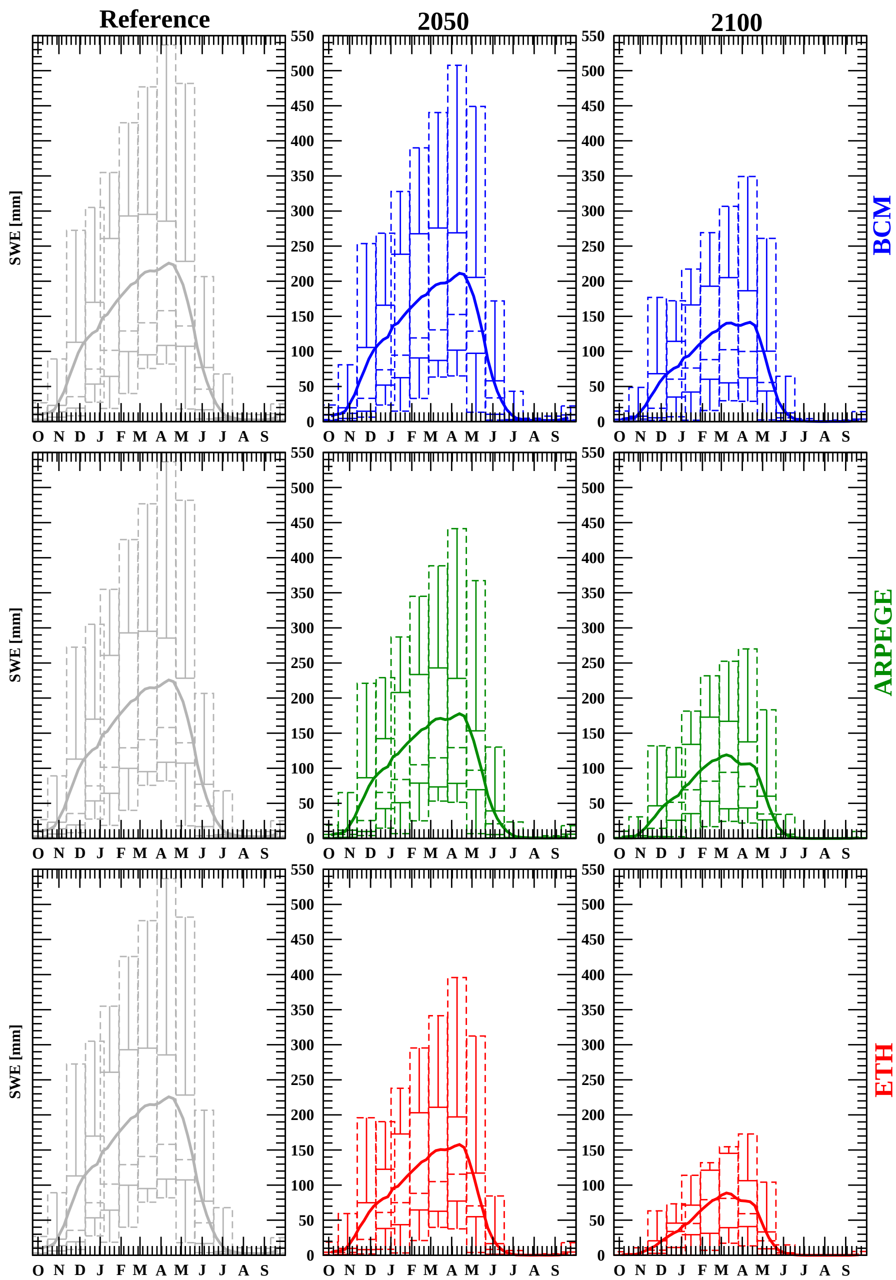

Figure 7: Development of Snow Water Equivalent for the whole domain for the reference, 2021-2050 and 2070-2095 scenarios. The thick line is the weekly average while the boxes represent the minimum, median, maximum as well as 25 % and 75 % quantiles.

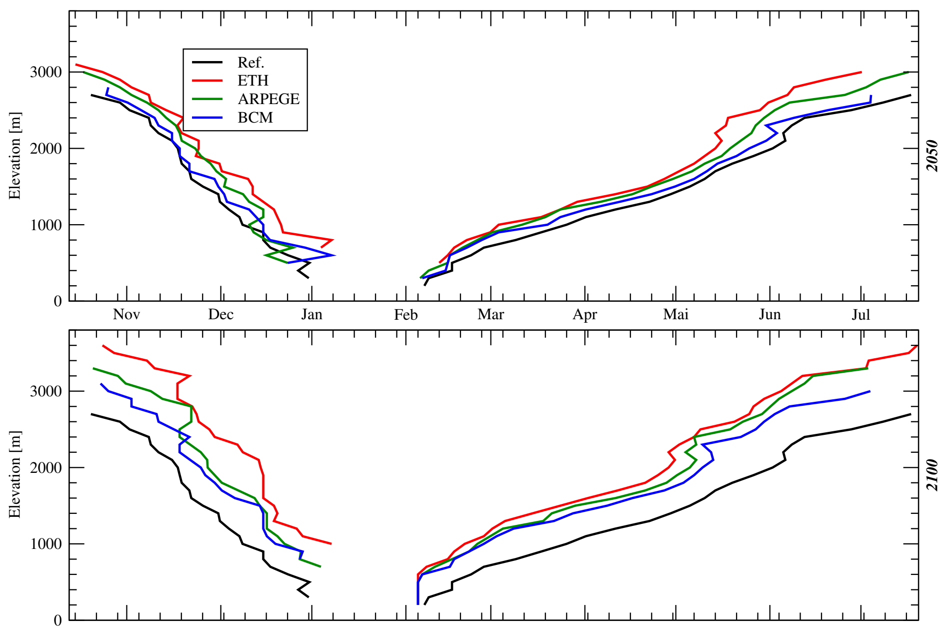

Figure 8: Snow season changes with elevation for the reference, 2021-2050 and 2070-2095 scenarios. The snow season is defined as continuously maintaining at least 10 mm of Snow Water Equivalent on average for a given 100 m elevation band.

3.2. Snow Season

When looking at SWE changes on Figure 7, a shift in the end of the snow season is visible: while in the reference scenario the snow melt ends in August, for the 2070-2095 period, in the worst case scenario, the snow melt would end mid-June. This becomes even more pronounced if we define the snow season as a period of continuous snow cover: then the impact of the various climate scenarios over the snow season duration can be evaluated. A threshold of 10 mm of SWE has been used to setup the plots in Figure 8 that show the beginning and the end of the snow season over the whole domain as a function of elevation using 100 m elevation bands. Practically, the latest point in time when the snow cover raises above the threshold defines the beginning of the snow season. Similarly, the first point in time when the snow cover decreases below the threshold defines the end of snow season.

From Figures 7 and 8, it can be concluded that the snow season would get shortened in future climate scenarios by 2-4 weeks for the 2021-2050 period and by 5-9 weeks for the 2070-2095 period. This is equivalent to an elevation shift of 200-400 m for the 2021-2050 period and of 400-800 m for the 2070-2095 period. This is consistent with the 900 m shift announced in Bavay et al. [8] for the A2 scenario for the period 2070-2095 for the Dischma catchment, which is also part of the current domain (although a very small part, see catchment 22 on Figure 5). As a consequence, because fall precipitation would shift in low elevations from snow fall (contributing to the SWE accumulation) to rain (immediately available for runoff), the snow season would get shorter with a potential for more flooding related to heavy rainstorms in the fall.

3.3. Runoff

We define runoff as the per pixel and per timestep flow made available for discharge out of a given soil column (by precipitation, snow melt or glacier melt). Note that no hydrological model is applied to account for storage effects and time transit of discharge. The reason for not using the Alpine3D routing scheme in this study is simply that the non-calibrated Alpine3D routing [14] is only suitable for smaller catchments and could not be used for the larger catchments treated in this study.

The runoff over the whole domain has been summed and classified by seasons in order to look at how runoff changes for the various scenarios defined in Table 5. Generally, runoff is increased in the winter and spring, for any scenario and period. In winter, an increase by 113 to 230 % is foreseen

2021-2050

	Winter	Spring	Summer	Fall	Tot.
BCM	44	5	-4	-3	-1
ARPEGE	45	12	-13	8	-2
ETH	99	3	-27	33	-7

2070-2095

	Winter	Spring	Summer	Fall	Tot.
BCM	144	12	-26	2	-9
ARPEGE	113	6	-38	6	-17
ETH	233	0	-43	37	-14

Table 5: Relative changes in runoff (in %), per season, for the whole domain for the 2021-2050 and 2070-2095 scenarios. No change shows as 0, while a positive change represents an increase and a negative change a decrease in runoff.

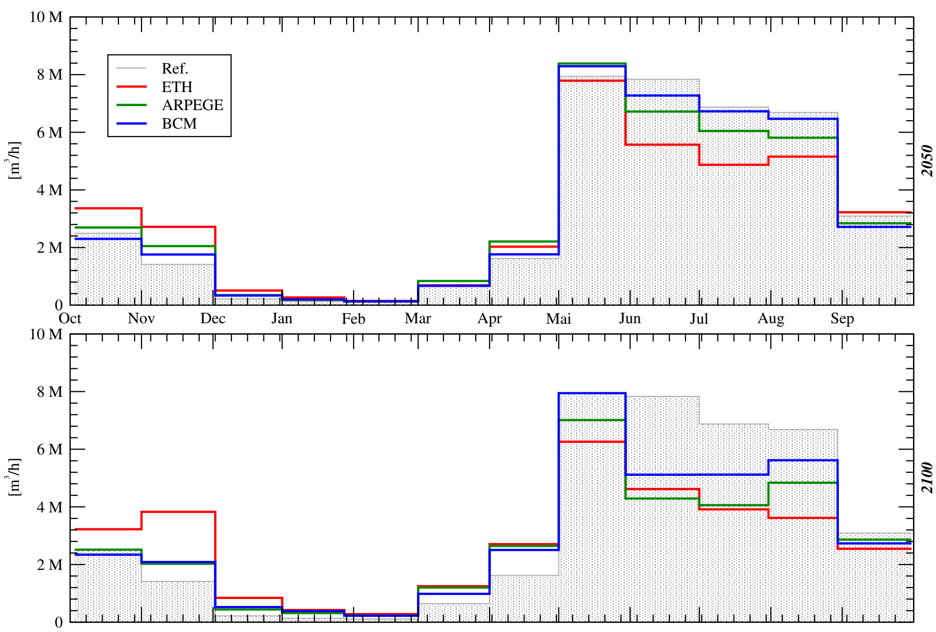

Figure 9: Changes in runoff for the whole domain for the reference, 2021-2050 and 2070-2095 scenarios. This does not represent catchment discharge but the amount of water that would be available in the domain, not taking into account temporal storage effects.

for the 2070-2095 period (44-99 % for the 2021-2050 period). This has to be understood in connection with the small runoff in winter in alpine catchments: the winter runoff is so low that a small absolute change produces a very large relative change. In spring, the increase would be more limited, in the 0-12 % range for the 2070-2095 period (3-12 % for the 2021-2050 period), but occurring at a time of high runoff. Smaller relative changes will also occur in the fall with a slight increase for the 2021-2050 period and up to a 37 % increase in the 2070-2095 period. In summer, on the other hand, runoff will be strongly reduced, in a period of generally high runoff, by 26 to 43 % for the 2070-2095 period (4-27 % for the 2021-2050 period). Over a whole year, the runoff would be reduced for all scenarios and both periods, as shown in Table 5. This is explained by reduced overall precipitation and increased overall evaporation. The modeled results also indicate a shift of the maximum annual runoff from summer towards spring.

These results are summarized in Figure 9 which can be interpreted as a non-calibrated discharge curve of the whole study domain. The largest fluctuations can be expected for the summer discharge with clearly lower absolute runoff and a time shifting of the peak flow. The increased winter discharge is also very distinct. This can be explained by an increasing number of melt events in the winter and by precipitation falling as rain instead of snow, due to the higher air temperatures.

3.3.1. Runoff composition

This section presents runoff generation in the three categories: precipitation, snow melt and glacier melt. The definition of these categories has been given in Section 2.3.3. Two areas have been selected from the whole domain to illustrate the impact of the various scenarios on two extreme cases: a high alpine headwater catchment and a low elevation section of a high order river. The first one (Roseggbach, catchment 21 in Figure 5) is a highly glaciated Inn headwater catchment (20 % of its surface being covered by glaciers) in the Engadine. Its lowest elevation is around 1800 m a.s.l and it goes up to 4049 m a.s.l. The other one is a section of the Alpine Rhine (sub-area 18 in Figure 5), that lies between 510 m a.s.l and 2805 m a.s.l. Only runoff generated in the selected sub-area has been accounted for, that is without any upstream hydrological discharge. Note that the contribution of glacier melt to total runoff in winter is usually an artefact, as explained in Section 3.3.

The Roseggbach area shows a clear effect of climate change (Figure 10). For the 2021-2050 period, the total runoff remains almost the same, but re-

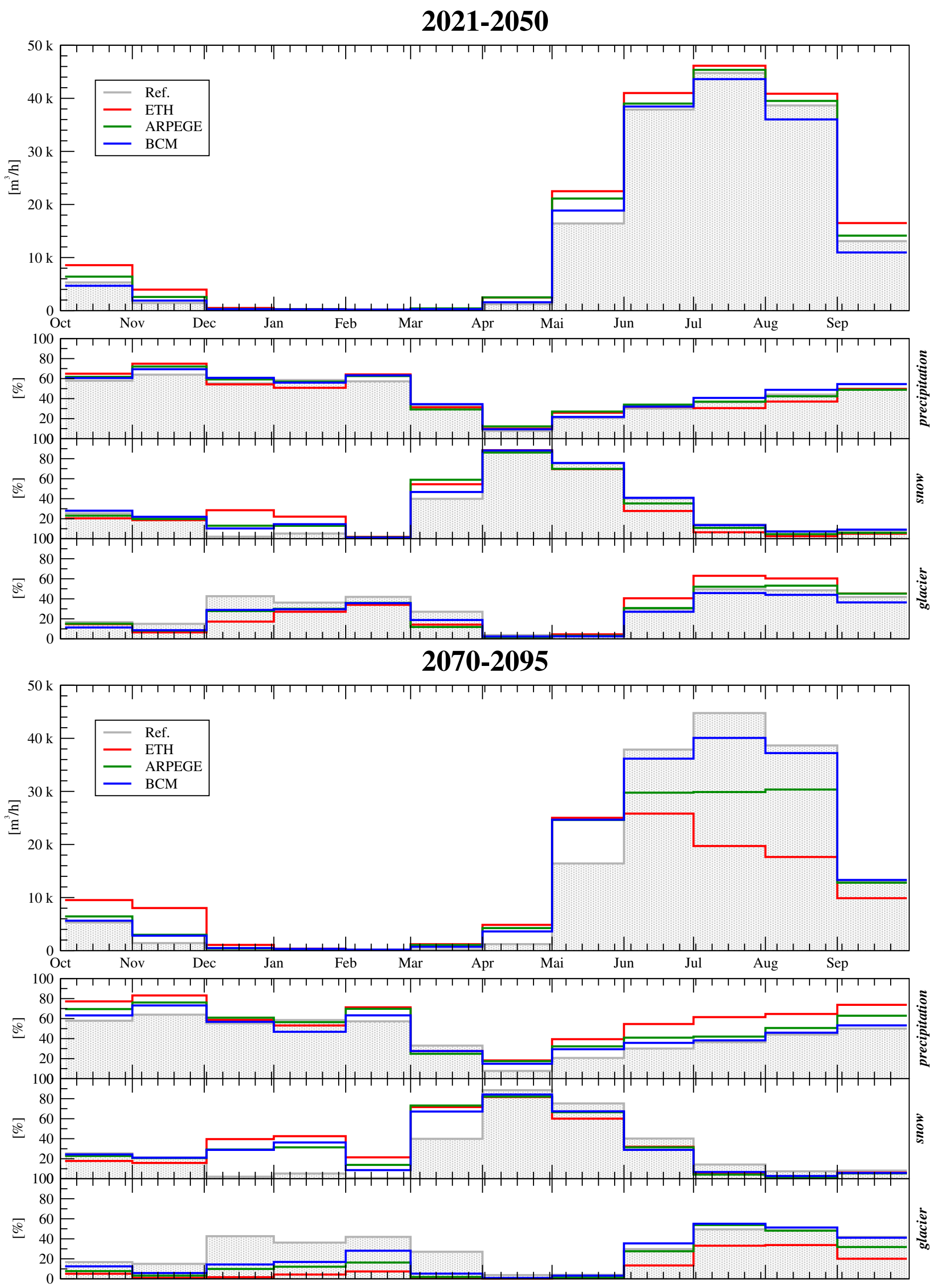

Figure 10: Changes in runoff and runoff origin for the Rosegbach (catchment 21, see Figure 5) for the reference, 2021-2050 and 2070-2095 scenarios. This does not represent catchment discharge but the amount of water that would be available in the domain, not taking into account temporal storage effects.

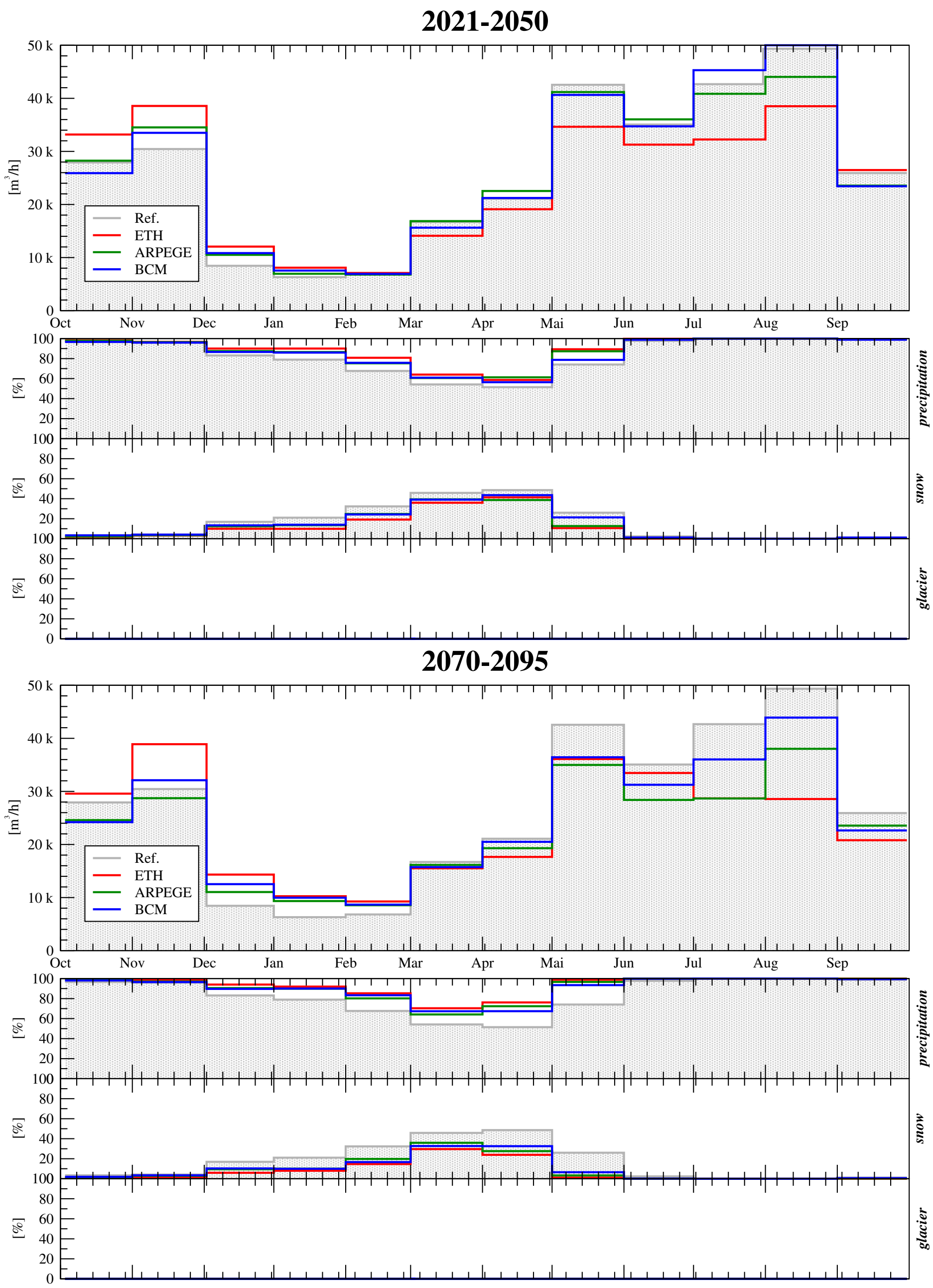

Figure 11: Changes in runoff and runoff origin for the Alpine Rhine (catchment 18, see Figure 5) for the reference, 2021-2050 and 2070-2095 scenarios. This does not represent catchment discharge as measured in the river but the amount of water that is available for the combined effect of groundwater recharge and runoff at every model pixel.

sults differ for the models: The BCM model shows a decrease while the ETH model shows a slight increase in average total runoff. This comes from an increase in summer glacier melt (June to September) that compensates the reduction of snow melt and summer precipitation (This is consistent with the findings of Stahl et al. [10]). In spring, the runoff is dominated by snow melt. For the 2070-2095 period, a clear decrease of the total runoff is visible for all scenarios. Moreover, the peak runoff is temporally shifted to an earlier time (here, one month earlier on these monthly accumulation plots). In the ETH scenario, because of the strong reduction of glacier coverage leading to a strong reduction in glacier melt contribution, the total runoff is strongly reduced. For other scenarios, the glacier melt is still able to contribute significantly to summer runoff, smoothing the total runoff reduction. The snow melt peak is also shifted by one month on these plots (as described in Section 2.2.3, each scenario has a matched glacier coverage map).

In contrast, the Alpine Rhine area only shows minor changes. For both periods, summer runoff is reduced, according to the reduction of precipitation (compare Figures 4 and 11). This area is not glaciated and therefore shows no glacier melt. However, a small reduction of snow melt can be seen, that can be compensated by an increase of the fraction of runoff coming from precipitation (for some scenarios, in March). This could partially be the effect of precipitation coming as rain instead of snow in the late winter/early spring.

These two extreme examples show how climate change effects are first smoothed and later amplified in melt-dominated areas while behaving much less drastically in precipitation-dominated areas.

4. Discussion and Conclusion

We presented model simulations of climate change impact on snow cover and runoff for a large mountainous area in the Swiss Alps. The domain covered more than $7200\,\mathrm{km}^2$ with a wide range of elevations: from highly glaciated elevations down to elevations where snow fall is relatively uncommon. The IPCC A1B emission scenario has been chosen and three different Regional Climate Models (RCM) have provided variations around this general scenario for two periods: 2021-2050 and 2070-2095. For the first period, the spread between the various RCM is greater than the difference between the reference period and the most moderate RCM; this is consistent with the findings of Rössler et al. [40]. Overall, the relative changes will be small for the next few decades. However, the second period shows much more significant changes and will transform snow dominated mountain catchment behavior fundamentally. Such changes include a shortening of the snow season by 5-9 weeks for the 2070-2095 period. This is roughly equivalent to an elevation shift of 400-800 m for the 2070-2095 period. The scenarios project a Snow Water Equivalents (SWE) reduction of up to two thirds towards the end of the century. A shift in the timing of the generated runoff is also envisioned: for all scenarios and all periods, spring and fall runoff will strongly increase, winter runoff would increase for some catchments (by a large relative value, but small absolute amount) while summer runoff will be dramatically decreased. The peak flow will also be shifted from summer toward late spring.

It is important to realize that these model projections have many possible uncertainties. One uncertainty is the error associated with the meteorological measurements per se and their potentially insufficient spatial coverage (Sevruk [41], Frei and Schär [42]) given the complexity of the terrain. Since we mainly focused on changes relative to the current state, these errors will to first order not influence the result and therefore we judge this error as being small compared to the uncertainty already represented by the different climate change models used.

Melt dominated, high alpine catchments will see a stronger temporal shift toward the spring with a strong reduction of summer runoff after significantly depleting glacier ice. This is consistent with the results of Stahl et al. [10]. Precipitation dominated catchments would become even more precipitation dominated with a small reduction in the spring melt that could be compensated by an increase of liquid precipitation. This means that initially highly glaciated areas would be able to compensate for a while by increasing glacial melt but would ultimately exhibit the most dramatic changes once most of the ice is gone, which will be the case by the end of the century.

Also with respect to runoff, we have chosen not to translate water production at individual grid points (here called runoff) to the conventional stream discharge because this step would introduce large uncertainties, which may affect the different time periods in a different way. The uncertainties would come from the fact that sub-surface processes in this type of terrain are both highly non-linear and inaccessible to physical modelling because not enough information is available on the structure of the sub-surface. Therefore, we present only water "production" in the vegetation, snow, ice, soil column for diverse sub-catchments but point out that these results are qualtitatively consistent with results obtained for conventional runoff predictions, including our own predictions e.g. for the Dischma catchment [8]. The precise timing of the stream flow will be different from the production as predicted here, especially for the larger catchments.

The effects of the future climate change has locally very strong implications: the reduction of snow season could have serious effects on tourism by depriving low elevation winter tourism resorts from reliable snow cover, the decrease of summer runoff would impact hydropower production and agriculture and the increase of spring discharge in alpine catchments could increase flooding risks downstream.

5. Acknowledgments

This work was performed as part of the Climate Change Adaptation by Spatial Planning in the Alpine Space (CLISP, http://www.clisp.eu) project, within the European Territorial Cooperation Alpine Space Project with funding from ETC Alpine Space Programme 2007-2013 and the Grisons Office for Spatial Development.

This work was also supported by the Swiss National Science Foundation and the AAA/SWITCH funded Swiss Multi Science Computing Grid project (http://www.smscg.ch) with computational infrastructure and support.

The authors would like to thank the many individuals who made this work possible, including Thomas Wüest from the Swiss Federal Institute for Forest, Snow and Landscape Research WSL, Boris Spycher and Christian Wilhelm from the office for Spatial Development Graubünden, Jan Magnusson, Nick Dawes and Florian Kobierska from SLF and Frank Paul from the Department of Geography of the University of Zurich.

References

[1] Matter MA, Garcia L, Fontane DG, Bledsoe B. Characterizing hydroclimatic variability in tributaries of the Upper Colorado River Basin–wy1911-2001. Journal of Hydrology 2010;380(3-4):260–76. doi: 10.1016/j.jhydrol.2009.10.040.

[2] Ragab R, Prudhomme C. Climate change and water resources management in arid and semi-arid regions: Prospective and challenges for the 21st century. Biosystems Engineering 2002;81(1):3–34. doi: 10.1006/bioe.2001.0013.

[3] Null SE, Viers JH, Mount JF. Hydrologic response and watershed sensitivity to climate warming in California's Sierra Nevada. PLoS ONE 2010;5(4). doi:10.1371/journal.pone.0009932.

[4] Rasmus S, Räisänen J, Lehning M. Estimating snow conditions in Finland in the late 21st century using the SNOWPACK model with regional climate scenario data as input. Annals of Glaciology 2004;38:238–44.

[5] Barnett TP, Adam JC, Lettenmaier DP. Potential impacts of a warming climate on water availability in snow dominated regions. Nature 2005;438:303–9. doi:10.1038/nature0414.

[6] Mote PW. Climate-driven variability and trends in mountain snowpack in westen North America. Journal of Climate 2006;19(23):6209–20.

[7] Hantel M, Hirtl-Wielke LM. Sensitivity of Alpine snow cover to European temperature. International Journal of Climatology 2007;27(10):1265–75.

[8] Bavay M, Lehning M, Jonas T, Löwe H. Simulations of future snow cover and discharge in Alpine headwater catchments. Hydrological Processes 2009;23:95–108. doi:10.1002/hyp.7195.

[9] Horton P, Schaefli B, Mezghani A, Hingray B, Musy A. Assessment of climate-change impacts on alpine discharge regimes with climate model uncertainty. Hydrological Processes 2006;20:2091–109.

[10] Stahl K, Moore RD, Shea JM, Hutchinson D, Cannon AJ. Coupled modelling of glacier and streamflow response to future climate scenarios. Water Resources Research 2008;44(2):1–13. doi:10.1029/2007WR005956.

[11] Magnusson J, Farinotti D, Jonas T, Bavay M. Quantitative evaluation of different hydrological modelling approaches in a partly glacierized Swiss watershed. Hydrological Processes 2010;25(13):2071–84. doi:10.1002/hyp.7958.

[12] Huss M, Farinotti D, Bauder A, Funk M. Modelling runoff from highly glacierized alpine drainage basins in a changing climate. Hydrological Processes 2008;3902:3888–902.

[13] Nolin AW, Phillippe J, Jefferson A, Lewis SL. Present-day and future contributions of glacier runoff to summertime flows in a Pacific Northwest watershed: Implications for water resources. Water Resources Research 2010;46. doi:10.1029/2009WR008968.

[14] Lehning M, Volksch I, Gustafsson D, Nguyen T, Stahli M, Zappa M. ALPINE3D: a detailed model of mountain surface processes and its application to snow hydrology. Hydrological Processes 2006;20:2111–28.

[15] Lundquist JD, Loheide II SP. How evaporative water losses vary between wet and dry water years as a function of elevation in the Sierra Nevada, California, and critical factors for modeling. Water Resources Research 2011;47. doi:10.1029/2010WR010050.

[16] Lehning M, Bartelt P, Brown RL, Russi T, Stöckli U, Zimmerli M. Snowpack model calculations for avalanche warning based upon a new network of weather and snow stations. Cold Regions Science and Technology 1999;30:145–57.

[17] Bavay M, Egger T. Meteoio: A meteorological data pre-processing library for numerical models. In: Geophysical Research Abstracts; vol. 13 of *EGU2011-11653*. EGU General Assembly 2011; 2011,URL `http://slfsmm.indefero.net/p/meteoio`.

[18] Marty Ch. Surface radiation, cloud forcing and greenhouse effect in the Alps. Ph.D. thesis; Eidgenössische Technische Hochschule Zürich; 2001.

[19] Liston GE, Elder K. A meteorological distribution system for high-resolution terrestrial modeling (micromet). Journal of Hydrometeorology 2006;7:217–34.

[20] Swiss Climate Change Scenarios CH2011. Zurich, Switzerland: C2SM, MeteoSwiss, ETH, NCCR Climate and OcCC; 2011. ISBN 978-3-033-03065-7. URL `http://www.ch2011.ch/`.

[21] Parry M, Canziani O, Palutikof J, van der Linden P, Hanson C, editors. Climate Change 2007: Impacts, Adaptation and Vulnerability. Contribution of Working Group II to the Fourth Assessment Report of the Intergovernmental Panel on Climate Change. Cambridge University Press; 2007.

[22] Graham LP, Hagemann S, Jaun S, Beniston M. On interpreting hydrological change from regional climate models. Climatic Change 2007;81:97–122. doi:10.1007/s10584-006-9217-0.

[23] Bosshard T, Kotlarski S, Ewen T, Schär C. Spectral representation of the annual cycle in the climate change signal. Hydrology and Earth System Sciences Discussions 2011;8(1):1161–92. doi:10.5194/hessd-8-1161-2011.

[24] Kobierska F, Jonas T, Magnusson J, Zappa M, Bavay M, Bernasconi SM. Future runoff from a partly glacierized watershed in Central Switzerland: a 2 model approach. Advances in Water Resources 2011;this issue.

[25] Paul F, Maisch M, Rothenbühler C, Hoelzle M, Haeberli W. Calculation and visualisation of future glacier extent in the Swiss Alps by means of hypsographic modelling. Global and Planetary Change 2007;55:343–57. doi:10.1016/j.gloplacha.2006.08.003.

[26] Swiss land use statistics 1992/97 - Nomenclature NOAS92: Basic categories and aggregations. Swiss Federal Statistical Office; 1992. URL `http://www.bfs.admin.ch`.

[27] Viviroli D, Zappa M, Gurtz J, Weingartner R. An introduction to the hydrological modelling system PREVAH and its pre- and post-processing tools. Environmental Modelling & Software 2009;24:1209–22. doi:10.1016/j.envsoft.2009.04.001.

[28] Groot Zwaaftink CD, Löwe H, Mott R, Bavay M, Lehning M. Drifting snow sublimation: A high-resolution 3-d model with temperature and moisture feedbacks. Journal of Geophysical Research 2011;116. doi: 10.1029/2011JD015754.

[29] Mott R, Schirmer M, Lehning M. Scaling properties of wind and snow depth distribution in an Alpine catchment. Journal of Geophysical Research 2011;116. doi:10.1029/2010JD014886.

[30] Lehning M, Löwe H, Ryser M, Raderschall N. Inhomogeneous precipitation distribution and snow transport in steep terrain. Water Resources Research 2008;44. doi:10.1029/2007WR006545.

[31] Mott R, Schirmer M, Bavay M, Grünewald T, Lehning M. Understanding snow-transport processes shaping the mountain snow-cover. The Cryosphere 2010;4(4):545–59. doi:10.5194/tc-4-545-2010.

[32] Helbig N, Löwe H, Lehning M. Radiosity approach for the shortwave surface radiation balance in complex terrain. Journal of the Atmospheric Sciences 2009;66:2900–12. doi:10.1175/2009JAS2940.1.

[33] Voelksch I, Lehning M. Model assessment of permafrost development for a large Alpine catchment. AGU Fall Meeting Abstracts 2005;.

[34] Luetschg M, Lehning M, Haeberli W. A sensitivity study of factors influencing warm/thin permafrost in the Alps. Journal of Glaciology 2008;54:696–704.

[35] Michlmayr G, Lehning M, Holzmann H, Koboltschnig G, Mott R, Schöner W, et al. Application of Alpine3D for glacier mass balance and runoff studies at Goldbergkees, Austria. Hydrological Processes 2008;doi:10.1002/hyp.7102.

[36] Fierz C, Lehning M. Assessment of the microstructure-based snow-cover model SNOWPACK: thermal and mechanical properties. Cold Regions Science and Technology 2001;33:123–31.

[37] Lehning M, Bartelt P, Brown RL, Fierz C, Satyawali P. A physical snowpack model for the Swiss avalanche warning. part ii. snow microstructure. Cold Regions Science and Technology 2002;35(3):147–67.

[38] Paterson WSB. The physics of glaciers. Pergamon; 3 ed.; 1994. ISBN 0-08-037944 3.

[39] Kuonen P, Bavay M, Lehning M. Pop-c++ and alpine3d: Petition for a new hpc approach. In: Asimakopoulou E, Bessis N, editors. Advanced ICTs for Disaster Management and Threat Detection: Collaborative and Distributed Frameworks. IGI Global; 2010, p. 237–61. doi:10.4018/978-1-61520-987-3.ch015.

[40] Rössler O, Diekkrüger B, Löffler J. Potential drought stress in a Swiss mountain catchment – ensemble forecasting of high mountain soil moisture reveals a drastic decrease, despite major uncertainties. Water Resources Research in press;doi:10.1029/2011WR011188.

[41] Sevruk B. Regional dependency of precipitation-altitude relationship in the Swiss Alps. Climatic Change 1997;36(3-4):355–69. doi:10.1023/A:1005302626066.

[42] Frei Ch, Schär Ch. A precipitation climatology of the Alps from high-resolution rain-gauge observations. International journal of Climatology 1998;18:873–900.